Responses of endothelial cells to extremely slow flows

Joong Yull Park,[1,2] Joshua B. White,[1] Natalie Walker,[3] Chuan-Hsien Kuo,[1] Wansik Cha,[1,3,a)] Mark E. Meyerhoff,[3] and Shuichi Takayama[1,b)]
[1]*Department of Biomedical Engineering, College of Engineering, University of Michigan, Ann Arbor, Michigan 48109, USA*
[2]*School of Mechanical Engineering, College of Engineering, Chung-Ang University, Seoul 156-756, Republic of Korea*
[3]*Department of Chemistry, College of Literature, Science, and the Arts, University of Michigan, Ann Arbor, Michigan 48109, USA*

(Received 5 January 2011; accepted 17 March 2011; published online 29 June 2011)

The process of blood vessel formation is accompanied by very minimal flow in the beginning, followed by increased flow rates once the vessel develops sufficiently. Many studies have been performed for endothelial cells at shear stress levels of $0.1-60$ dyn/cm^2; however, little is known about the effect of extremely slow flows (shear stress levels of $10^{-4}-10^{-2}$ dyn/cm^2) that endothelial cells may experience during early blood vessel formation where flow-sensing by indirect mass transport sensing rather than through mechanoreceptor sensing mechanisms would become more important. Here, we show that extremely low flows enhance proliferation, adherens junction protein localization, and nitric oxide secretion of endothelial cells, but do not induce actin filament reorganization. The responses of endothelial cells in different flow microenvironments need more attention because increasing evidence shows that endothelial cell behaviors at the extremely slow flow regimes cannot be linearly extrapolated from observations at faster flow rates. The devices and methods described here provide a useful platform for such studies.
 [doi:10.1063/1.3576932]

I. INTRODUCTION

Vascular endothelial cells (ECs) are highly shear stress-sensitive. Physiologic fluid flows in the ranges of about $1-50$ dyn/cm^2 are found in the majority of blood vessels, and the disturbance of this flow can lead to pathogenic states such as atherosclerosis and thrombosis.[1,2] Although shear is higher in larger vessels, for some microcirculation[3] processes, shear stress as low as 0.1 dyn/cm^2 has been reported.[4,5] Flows that give shear stress below 0.1 dyn/cm^2 also exist physiologically[6–8] and are also expected to affect functions such as cell morphogenesis and pathogenesis of lymphatic diseases.[6] However, the lowest end of this spectrum, corresponding to shear stress levels of $\sim 10^{-2}-10^{-4}$ dyn/cm^2, has not been studied. This is in part due to the lack of a convenient and reliable method to generate such slow flows. There are reports of exposing ECs embedded in hydrogel to interstitial flow (a few tens of μm/s);[9,10] however, the focus was on EC invasion into the interstitium. Therefore, there is a need of a different method that allows us to have slow flows in luminal capillary-like structure with extremely slow and controlled flows.

Two different flow sensing mechanisms of EC are generally accepted.[11,12] In direct sensing, transmembrane mechanoreceptors in EC luminal and abluminal membranes directly sense shear stress through physical deformation, which relays signaling to cytoskeletal proteins and focal adhesions (see Fig. S1a in the supplementary information[13]).[3,12] In the indirect mechanism of flow

a)Present address: Nuclear Chemistry Research Division, Korea Atomic Energy Research Institute, P.O. Box 105, Yuseong, Daejeon 305-535, Republic of Korea.
b)Author to whom correspondence should be addressed. Tel.: 734-615-5539. FAX: 734-936-1905. Electronic mail: takayama@umich.edu.

sensing, surface receptors sense changes in concentration of ligands. Therefore, flow rate is sensed indirectly via the change in ligand concentration based on mass transfer properties (Fig. S1b in the supplementary information[13]).[12] Distinguishing between the direct and indirect mechanisms of flow sensing is difficult, particularly with the high flow rates reported in previous literature.

Here, we utilize a previously reported osmotic pump[14–16] to generate the required extremely slow flows over ECs attached to the surface of a microfluidic channel rather than embedded in hydrogels and analyze their responses; modeling the internal lumen of developing blood vessel. Slow flows with extremely low shear stresses ($10^{-2}-10^{-4}$ dyn/cm^2), which cover a diffusion-dominant flow regime which is useful for evaluating the role of the indirect mechanism, were achieved and applied to the single layered endothelial cells. To characterize the cellular responses, the experiments were designed and performed to derive three biological readouts: proliferation, adherens junction development, actin structure, and nitric oxide (NO) production. Angiogenesis is a locally confined event and dependent not only on global cues (growth factor or other chemical soluble factors) but also local cues (ECM or other mechanical cues);[17,18] however, knowing that NO is also a local cue (lifetime of 5 s) and an important angiogenesis-modulator, NO secretion from ECs exposed to extremely low flow in newly sprouting capillary is interesting to analyze. Adherens junction is a mediator for stabilization signals in EC monolayers and reduces sprouting.[19] Proliferation is a basic parameter for general cellular studies; however, EC proliferation is particularly important in angiogenesis due to its dependency on NO concentration and adherens junction development. By analyzing these responses at extremely slow flow levels, we aimed to better understand EC behavior in negligible shear stress in slow flow regimes as might be found in conditions such as vessel sprout formation.

II. MATERIALS AND METHODS

A. Microfluidic system design

We fabricated the microchannel using a conventional soft lithographic process using polydimethysiloxane (PDMS) (Dow Corning, Midland, MI). The main channel was 200 μm in height, 5 mm in width, and 20 mm in length (Fig. 1). Flow was generated by osmotic pumps and the flow rate was controlled by altering concentrations of polyethylene glycol (PEG) (Sigma-Aldrich, St. Louis, MO) in aqueous solution:[14–16] briefly, PDMS cubic chambers (inner space of $5\times5\times5$ mm) with a window of cellulose membrane (5×5 mm, used as the osmotic membrane) were connected to tubing and filled with de-ionized (DI) water. An osmotic pressure was generated as a result of the solute differential between the inner chamber filled with water and the outer chamber filled with PEG solution, resulting in flow. In our osmotic pump setup, the flow rate ($Q=-\alpha AL_P\Delta\pi$, where α is reflection coefficient, A is contact area of membrane, L_P is hydraulic permeability, and π is osmotic pressure) is a linear function of the mole concentration C based on $\pi=CRT$, where R is gas constant and T is absolute temperature.[20] The linear relationship of concentration and flow rate was shown previously.[14] In addition, it is good to note that the osmotic pressure used in our system is far greater than the possible resistance of the air bubble trapped intentionally in the tubing (Fig. 1). Micropipette tips (1 ml) were used as the inlet reservoir and maintained for 24 h. Sample solutions containing cell-secreted factors were collected in the commercial polyurethane tubing (OD of 2 mm, ID of 1.2 mm) (TU0221C-020, Pneuaire Co., CA) downstream of the chamber as drainage occurred by osmotic pump. To ensure the channel flow was not affected by evaporation, the experimental setup was placed within plastic case in which extra water reservoirs were provided; additionally, the micropipette tips were covered and the microdevices were initially wet.

B. Computational two–dimensional model

For supportive study, a simple two-dimensional (2D) capillary model was used to describe how much the shear stress can be reduced in sprouting capillary branches. As shown in Fig. 2, the length of the branching sprout was modeled with lengths L and 2.5xL where L is the width of the main capillary. The dimension, velocity, and other parameters were chosen to give a Reynolds

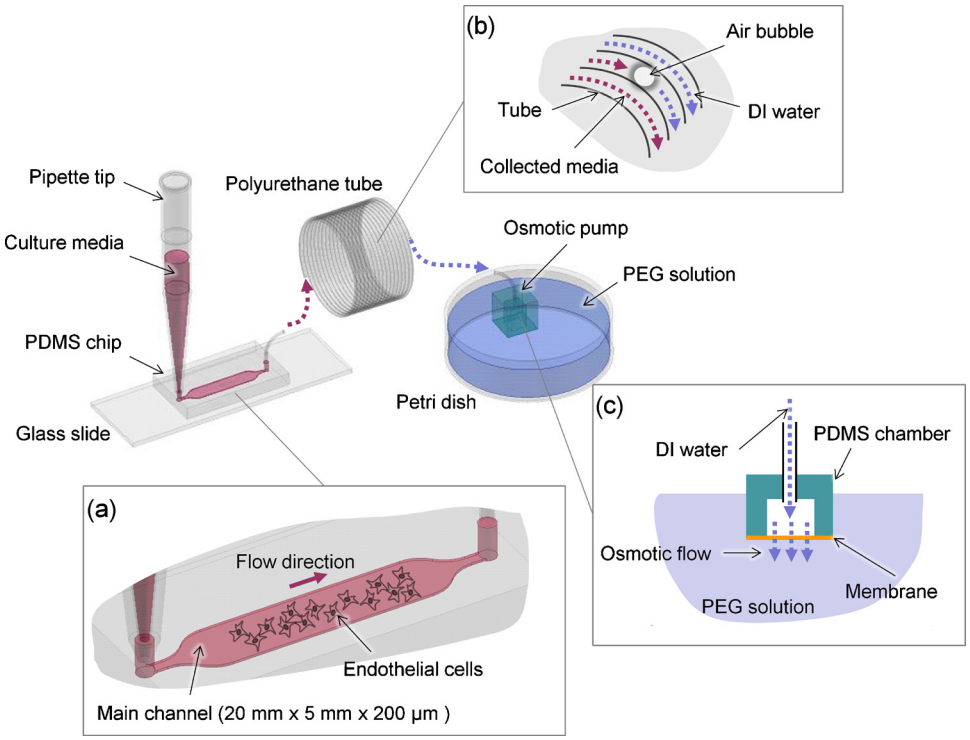

FIG. 1. System setup consists of a pipette tip, a microchip on a glass slide, a coiled PU tube for collecting media, an osmotic pump unit, and PEG solution in a Petri dish. (a) The main channel has dimensions of 200 μm in height, 5 mm in width, and 20 mm in length. Culture media in the pipette tip slowly flow into the main channel of the chip where ECs are cultured. (b) PU tube primed with DI water connects the microchannel and the osmotic pump unit. A small air bubble is inserted intentionally to prevent mixing of collected media and DI water. (c) Osmosis occurs due to the concentration difference between PEG solution and the DI water in the osmotic pump unit through the water-permeable cellophane membrane.

number of typical capillary flow ($\sim 10^{-13}$, assuming blood's dynamic viscosity is 0.000 79 kg/m s, density is 993 kg/m^3, blood flow velocity is 10^{-3} m/s, and capillary diameter is 100 μm). Conventional incompressible Navier–Stokes equation was calculated on the modeled computational domain constructed with the triangular mesh (element number of mesh $\sim$1600–1800). Calculation was regarded to be converged when the residual reached 10^{-9}. COMSOL Multiphysics 3.4 (COMSOL Inc., Los Angeles, CA) was used for simulation.

C. Cell culture and staining

Prior to cell seeding, the microchannels were coated with fibronectin (100 μg/ml) for 2 h and washed with phosphate buffer solution (PBS). Human umbilical vein endothelial cells (HUVEC) were seeded at a density of 4×10^6/ml. After allowing stabilization and proliferation of cells (toward desired confluence of 80%, left, Fig. 3) for 24 h in the incubator, slow flow was applied to HUVEC layers. Two control devices were incubated without applying flow. After 24 h of perfusion, all devices were disconnected from osmotic pumps and the cell monolayers were fixed with 4% paraformaldehyde solution for 10 min at room temperature and permeabilized using 0.5% Triton X-100 solution (in PBS). Junction staining was performed by incubating 0.8 μg/ml VE-cadherin antibody (C-19, Santa Cruz Biotechnology, Santa Cruz, CA), then the samples were treated with 2 μg/ml Alexa Fluor® 488 conjugated donkey anti-goat IgG secondary antibody (Invitrogen, Carlsbad, CA) for 1 h at room temperature. Actin staining was performed by incubating the samples with 0.165 μM solution of Alexa Fluor 594-conjugated Phalloidin (Invitrogen); all steps were followed by PBS wash. Stained samples were observed under a fluorescence microscope (TE300, Nikon, Melville, NY) equipped with Digital Camera (Hamamatsu, Bridge-

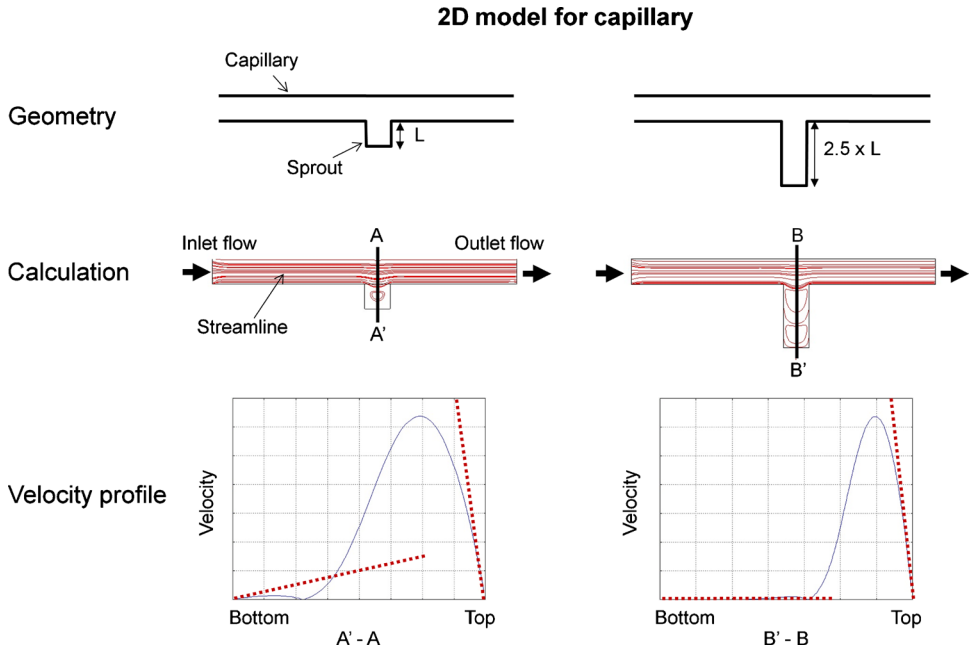

FIG. 2. Computational fluid dynamic model for capillary sprout. Top: Capillary geometry was constructed in 2D with two different branching sprouts (L and 2.5×L). Middle: Calculated flow field in capillary model shows recirculation in the geometry. A-A′ and B-B′ are cross-lines at which velocity profiles were derived. Bottom: Velocity profile in the short branch model (l) shows significant differences in magnitudes (~30 times) of velocity gradients (shown as dotted lines), and moreover, the long branch model (2.5×L) has a negligible velocity gradient at the tip of the capillary sprout.

water, NJ) and SimplePCI (Hamamatsu) imaging software. Staining was done on the same day and concentrations of chemicals and exposure times were constant for all experiments.

To quantify the amount of adherens junction, we measured pixel numbers of adherens junction within the designated area from images of each flow condition including static culture control. The raw area pixel values from the adherens junction staining images were divided by both cell count and cell area to produce a normalized data set of cell number/area-independent values to account for the density differences from different samples.

D. Detection of cell-secreted nitric oxide

In our study, we used a Sievers NO Analyzer 280i (GE Analytical, Boulder, CO) to measure the NO concentration in the collected samples from the perfusion microsystems. When cells secrete NO in solution, it is highly unstable and quickly oxidized to nitrite in the presence of O_2 according to second order reaction kinetics,

$$2NO + O_2 \rightarrow 2NO_2,$$

$$2NO + 2NO_2 \rightarrow 2N_2O_3,$$

$$2N_2O_3 + 2H_2O \rightarrow 4NO_2^- + 4H^+.$$

Therefore, solutions collected from the sample tubing actually contain nitrite instead of NO. To determine the amount of NO actually secreted by cells, it is necessary to convert the nitrite back into NO. This is accomplished by injecting sample solution into the NOA, where the nitrite in the sample reacts with 0.6 M KI and 0.1 M H_2SO_4 according to the following reaction:

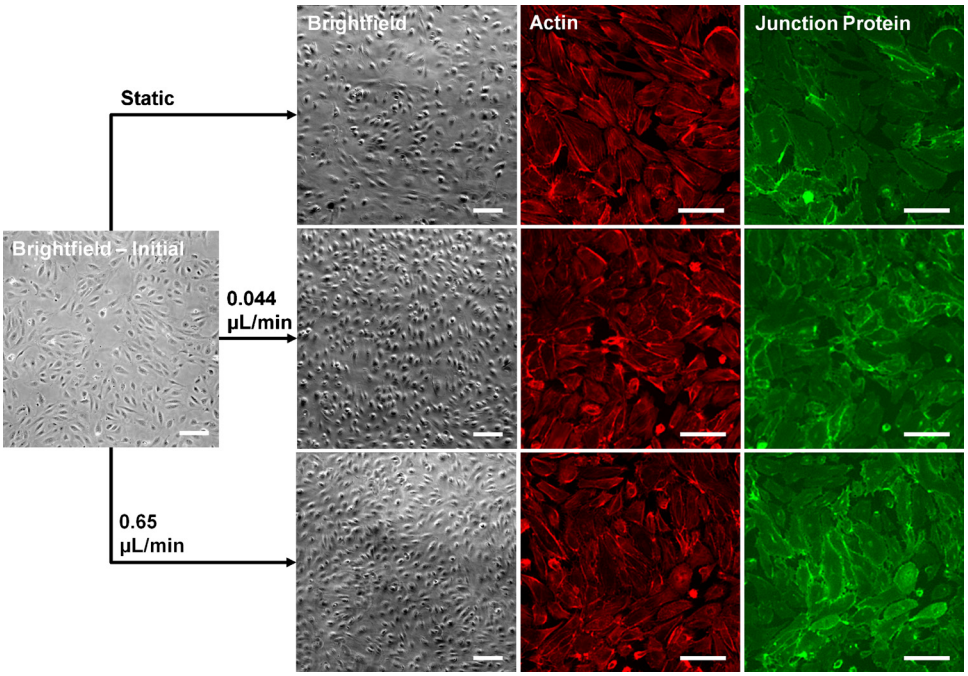

FIG. 3. Cell images taken after 1 day for stabilizing and another 1 day for perfusion/static culture. Three different conditions were compared: static culture, slowest flow (0.044 μl/min) culture, and fastest flow (0.65 μl/min) culture. Brightfield images (left column) show there is significant difference in cell density between static control group and flow groups. Cytoskeletal structures by actin staining (red, center column) in each group show no evidence of reorganization (random directionality). However, adherens junction staining images (green, right column) show meaningful difference in intensity; regardless of cell density, adherens junction of ECs in static culture are less developed compared to ECs in the flow groups. Scale bars are 100 μm.

$$2I^- + 2NO_2^- + 4H^+ \rightarrow I_2 + 2NO + 2H_2O.$$

Finally, once nitrite has been converted back into NO, it reacts with ozone to produce nitrogen dioxide and a photon of light.

Culture media were continually perfused through the microchannel at fixed flow rates for 24 h. After 24 h, polyurethane tubing containing culture media with cell-secreted factors (from cell-culture devices) and tubing containing only culture media (from devices without cells) were detached from the devices. The collected sample solutions were then transferred to 1.5 ml microcentrifuge tubes and frozen. Before testing, tubes were thawed, then injected via gas-tight syringe into a sample cell containing potassium iodide (KI) and sulfuric acid (H_2SO_4) at final concentrations of 0.6 M and 0.1 M, respectively. The nitrite in the sample solutions reacts with the KI and H_2SO_4 to produce NO. The amount of NO is then detected by chemiluminescence in a Sievers Nitric Oxide Analyzer (NOA) 280i (GE Analytical, Boulder, CO).

III. RESULTS AND DISCUSSION

A. Slow perfusion flow characterization

Osmotic-pressure-controlled flow was applied for 24 h at calculated flow rates of 0.044, 0.19, 0.31, and 0.65 μl/min based on volumetric displacement measurements. The typical aspect ratio of the cross-sectional area of the main channel was 0.04, such that the flow can be assumed to be parallel-plate *Poiseuille* flow; and the equation relating wall shear stress (τ_w) to channel dimensions is $\tau_w = 6\ \mu Q/h^2 w$, where Q is volumetric flow rate, h is channel height (=200 μm), and w is channel width (=5 mm). The dynamic viscosity of culture medium, μ is 0.000 785 kg/m s (1.04 times higher than water) at 37 °C.[21,22] Shear stress values were calculated as 1.69×10^{-4}, 7.46×10^{-4}, 1.22×10^{-3}, and 2.55×10^{-3} dyn/cm^2 in respect to four applied flow rates, which are over

hundreds times smaller than those in previously reported experiments ($0.1-1$ dyn/cm^2).[3–5,23]

2D computational study allowed us to have an intuitive physical data about how much reduction of flow power can be made at the tip of branching channel. Streamlines in sprouts showed recirculating flow that contributes to reduced shear forces. Velocity profiles were derived for A-A′ and B-B′ in Fig. 2. Steep velocity gradients occur near the wall in the main channel for both models, while velocity gradients are very low (about 30 times smaller) for the model having a short (L) sprout and almost zero for the model having a long ($2.5\times$L) sprout. Because velocity gradients are linearly proportional to shear stress, this also implies a minimal amount of wall shear stress at the tips of the sprouting branch. Although capillaries and sprouts are cylindrical and have a range of cross-sectional areas *in vivo*, our simple computational model suggests that convective flow and shear stress at the tip of the sprouting capillary may be extremely small.

B. Cell morphology and staining

We double-stained actin fibers and VE-Cadherin proteins on the EC monolayer of each device. Brightfield and immunofluorescence images of actin and adherens junction were acquired and overlaid for image analysis (Fig. 3). As shown for actin staining images (*center column*, Fig. 3), no evidence of EC alignment was found in any groups. This fact supports the notion that the flow levels used in this study were too small to trigger cytoskeletal reconstruction which is mediated by the direct shear-sensing mechanism of ECs.[24,25] Low physiological shear stresses are found in microcirculation which is about 0.1 dyn/cm^2,[4,5] and our results on shear stress ranged from 1.69×10^{-4} dyn/cm^2 (0.044 μl/min) to 2.55×10^{-3} dyn/cm^2 (0.65 μl/min), which is over a hundred times lower and might be a direct reason why the cytoskeletal rearrangement was not triggered. When diffusion becomes a major role in transportation of molecules, the responses from cells under such slow flows might be more related to indirect flow-sensing mechanisms. To show the relative importance of diffusion in the generated flows, we estimated the Péclet number (Pe), a dimensionless number for the ratio of convection to diffusion, and found that it ranges from 0.2 at the slowest flow rate (0.044 μl/min) to 3 for the highest flow rate (0.65 μl/min) in our study. After 24 h under slow flows, the cell density in the flow groups was significantly higher than the static control group [Fig. 4(a)]. This result seemingly contradicts previously well-known studies where shear stress inhibits EC proliferation at physiological blood flow levels in matured vessels.[26] However, more recent studies found that EC proliferation is encouraged by slow interstitial flows (velocity of about 10 μm/min), and beyond this very slow flow regime, EC proliferation starts to decrease with increasing flows.[9,10] Although these previous studies are not directly comparable to our system due to three-dimensional (3D) geometries and impeded flow features, it aligns well with the our finding that blood flow does not always inhibit EC proliferation but can enhance it according to the flow magnitude. Thus, these findings further emphasize why EC response toward extremely slow flow rates needs to be studied separately from higher flow levels. We did not find the evidence of apoptosis in this experiment.

In addition to enhanced proliferation, adherens junction formation, which is important for EC monolayer integrity,[20] was also higher in the four flow groups [Fig. 4(b)]. The cell spreading area, on the other hand, was lower in the flow groups compared to static control [Fig. 4(a)] again consistent with vessel stabilization and junction protein development in confluent cells.[19,27]

C. EC NO production

Angiogenesis, including capillary sprout formation, requires vasodilation and increased vascular permeability, for which NO plays an important role.[28] We measured EC NO secretion levels to investigate the EC vasoregulatory function under slow flows. It is important to note that previous reports have shown that NO secretion is not a first order linear function of shear stress in the range of $1-10$ dyn/cm^2,[5] and thus we cannot simply extrapolate previously obtained results to estimate NO secretion at our low shear levels. We measured the NO level of each device and then normalized the NO measurements to control devices without cells to account for basal levels of nitrite found in culture medium. We converted the measured NO concentrations to number of NO

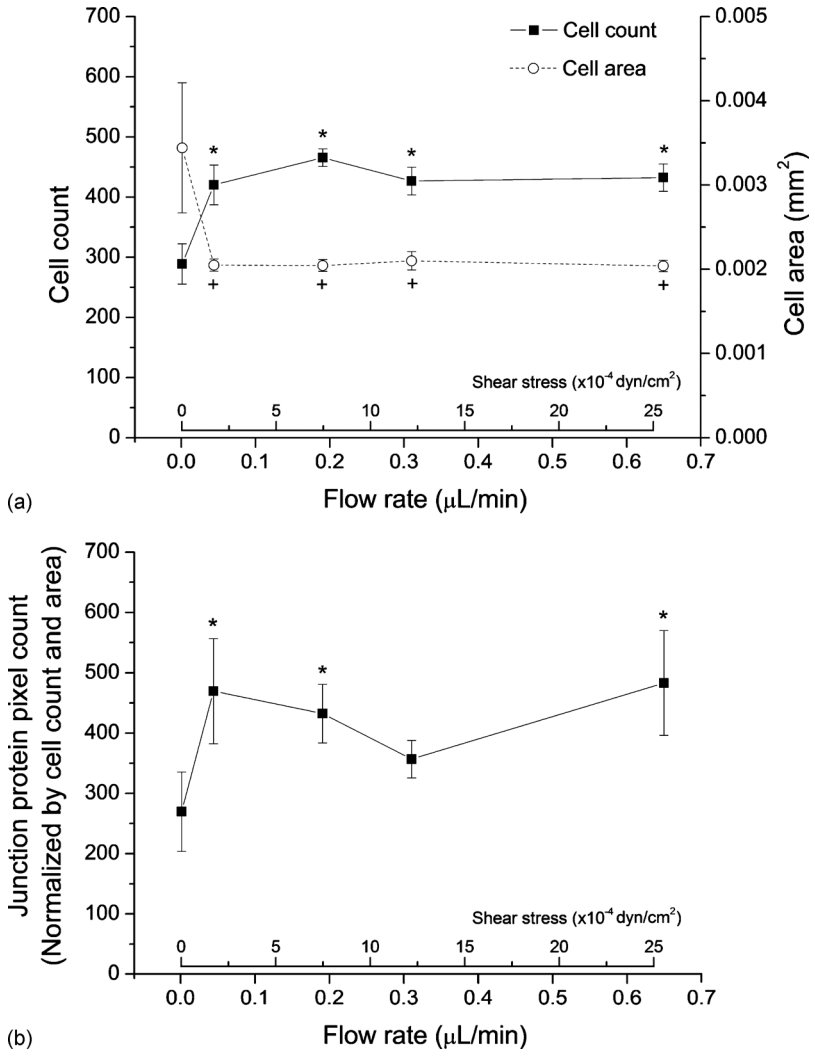

FIG. 4. Cell proliferation and adherens junction measurement. The data were derived from the images taken at five randomly chosen locations in each sample, and each image size was 800×800 μm. (a) The cells in each device were counted and analyzed for the designated spreading area of the cells. It was clearly shown that the perfusion culture enhanced cell proliferation during 2 days of culture, while cells in static culture devices were more spread. (b) Adherens junction was measured by counting pixels in the corresponding images. Normalization was required because the cell density and spreading area were different particularly between static control and flow groups; for this, measured adherens junction pixels were divided by both cell count and spreading area. Values are expressed as mean $\pm$ SD $^{*}p$ and $^{+}p < 0.05$ vs static culture.

molecules using corresponding sample volume; this was done because flow rates vary across devices so absolute numbers of NO molecules is a more objective readout. In Fig. 5(a), squares represent the measured number of NO molecules in the collected medium from cell culture devices, while circles show measured NO in medium collected from devices without cells. Measured numbers of NO molecules from cell-less devices increase linearly with flow rate because background NOx species (oxidized nitrogen) in environmental air surrounding the chamber, which is partitioning favorably into the PDMS matrix of the device, get into the media and are interpreted as NO molecules in the measuring device (Sievers NO Analyzer 280i). At lower rates, more gas molecules get into the solution but the flux slows somewhat because of the concentration increase in the solution phase with time. However, at higher flow rates, more fresh media flows through the device, maintaining a higher concentration gradient and therefore flux of NOx species

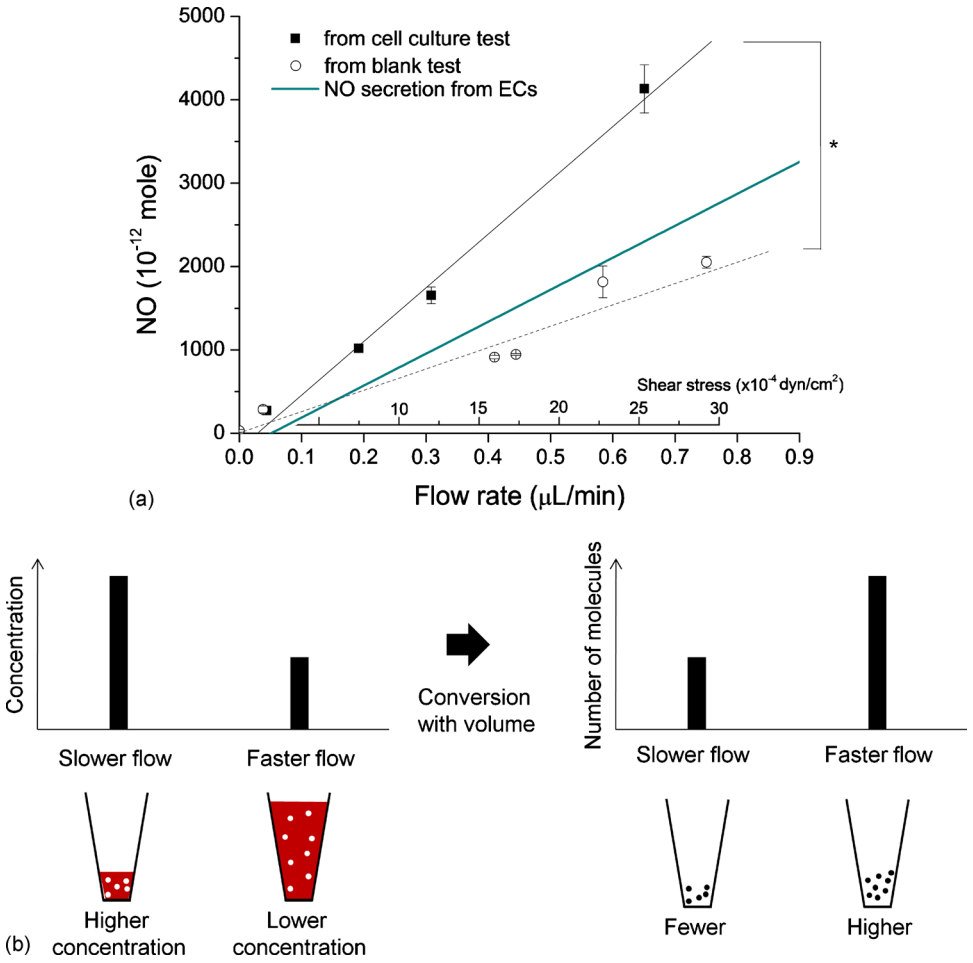

FIG. 5. (a) NO secretion level. The media perfused through the microchannel were collected in the tube (tube connects osmotic pump and microchip) and analyzed to derive number of NO molecules in the collected sample. In the graph, dark square marks represent the numbers of NO molecules in each cell culture devices, and data were fitted to a line (solid line). Meanwhile, circles represent the number of NO molecules derived from blank media perfusion experiments with the same microchip devices (linear fit in a dashed line); without cells, the nitrite from the atmosphere interacts with the perfusion media due to the permeability of PDMS, and this should be subtracted from the data derived from cell culture devices. Then, the final graph was derived, represented in green solid line. Data points are expressed as mean ± SD and $^{*}p < 0.01$. (b) In the microchannel, atmospheric nitric gas molecules dissolve in the media due to the high surface area to volume ratio of microfluidics and gas permeability of PDMS. The amount of trapped NO depends on flow rate: high flow rates produce large sample volumes which absorb more total NO; conversely, slow flow rates produce smaller sample volumes with higher concentrations of NO. Slow flows have higher concentrations because the medium remains in the device longer, therefore, it is exposed to atmospheric gas longer which allows more gas to diffuse into the medium (and results in higher concentrations).

into the device over time. Hence, while the concentration of total NO in the solution is less at higher flow rates, the measured total number of NO molecules in each collected total volume shows the increase with increasing flow rate [Fig. 5(b)]. Consequently, more gas diffuses into the media and contributes to higher background NO. We subtracted the background data from the cell culture data to derive the real NO secretion data from ECs [green line, Fig. 5(a)]. The plot shows ECs actively secrete NO molecules with increasing levels of shear, even at these slow flows, and the relationship between NO secretion and flow rate appears linear. Previous literature suggests that ATP is released from ECs to act on purinoreceptors that eventually trigger endothlelium-derived relaxing factor release, such as NO.[29] Our results are consistent with this kind of ligand receptor-mediated mass transport sensing mechanism that enables ECs to sense slow flows at

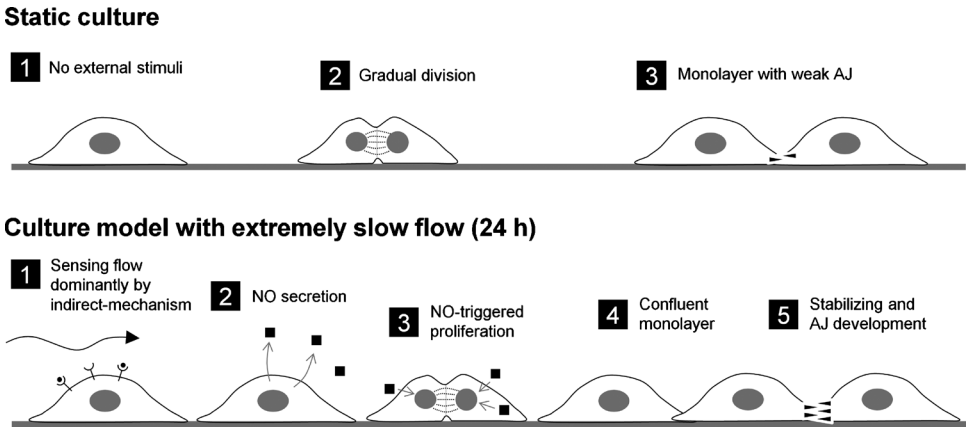

FIG. 6. Comparison between static control and flow groups. In static culture group (top), no flow stimulus was applied to observe that ECs proliferated gradually to achieve a monolayer in 48 h of culture with weak adherens junction development. Meanwhile in EC culture group with extremely slow flow (bottom), a confluent monolayer formed with well-developed adherens junction. It seems even extremely slow flow can trigger EC responses including NO secretion to enhance proliferation and make the cells progress to a stable state with strong adherens junction development.

which direct shear-sensing mechanism is not triggered.[29,30] This report, however, is the first time actual quantified data have been obtained at these extremely slow flow rates.

D. Hypothesis on extremely low shear effect to EC

From the above-mentioned results together with literature data, a hypothesis can be produced as following: during vessel development, the sprouting vessel tips are at site of extremely limited flow. ECs in such regions, however, still can sense mass transport and prepare themselves in anticipation of subsequent higher flow conditions to come. Thus, the cells, at least in part aided by increased NO production, increase proliferation resulting in higher confluence of cells and increasing junction protein expression while cytoskeletal reorganization does not occur until subsequent exposure to higher shear stress that triggers mechanoreceptors. This matches the general four step sprouting angiogenesis scheme (Fig. 6). First, dissolution of adherens junction to increase permeability. Second, cell proliferation near the target area. Third, cell invasion. Finally, a capillary channel forms and adherens junction redevelop. Static conditions maintain ECs in the early steps, whereas even slow flow pushes the cells toward the latter steps. In addition to the potential physiological relevance and importance of these findings, these results give guidance for performing *in vitro* microfluidic endothelial cell culture studies. There are anecdotal notes of the need of slow perfusion for endothelial cell growth in microchannels but much more detailed evaluations seem necessary.[31,32]

IV. CONCLUSIONS

This paper compared EC cultures with extremely slow level of flows with static conditions. We showed that slow flows with extremely low shear stress can still enhance EC proliferation and adherens junction development, but do not modify cytoskeletal structures. The results and methods described here provide useful insights and tools for studying the role of slow flows and endothelial cell culture experiments. In addition, the osmotic pumping system used in our study is a modular component which can be easily combined with other microfluidic systems and extended to further cellular studies including not only endothelial cells but also other cell types such as neuronal cells where extremely slow flows are physiologically relevant.

ACKNOWLEDGMENTS

The authors express thanks to James Dalrymple and Dr. Mark Lindsay for their help in statistical analysis. This work was supported by the NIH (Grant No. HL-084370) and the Coulter Foundation. The measurements of NO secretion in MEM's laboratory were supported by the NIH (Grant No. EB-000783). J.B.W. is supported by the National Science Foundation through a Graduate Research Fellowship (Grant No. 2010101926) and University of Michigan Rackham Merit Fellowship.

[1] A. E. Silver and J. A. Vita, Circulation **113**, 2787 (2006).
[2] O. Traub and B. C. Berk, Arterioscler., Thromb., Vasc. Biol. **18**, 677 (1998).
[3] P. F. Davies, Physiol. Rev. **75**, 519 (1995).
[4] D. Kaiser, M. A. Freyberg, and P. Friedl, Biochem. Biophys. Res. Commun. **231**, 586 (1997).
[5] A. J. Kanai, H. C. Strauss, G. A. Truskey, A. L. Crews, S. Grunfeld, and T. Malinski, Circ. Res. **77**, 284 (1995).
[6] M. A. Swartz and M. E. Fleury, Annu. Rev. Biomed. Eng. **9**, 229 (2007).
[7] J. M. Rutkowski and M. A. Swartz, Trends Cell Biol. **17**, 44 (2007).
[8] K. Yamamoto, T. Sokabe, T. Watabe, K. Miyazono, J. K. Yamashita, S. Obi, N. Ohura, A. Matsushita, A. Kamiya, and J. Ando, Am. J. Physiol. Heart Circ. Physiol. **288**, H1915 (2004).
[9] C. E. Semino, R. D. Kamm, and D. A. Lauffenburger, Exp. Cell Res. **312**, 289 (2006).
[10] R. Hernández Vera, E. Genove, L. Alvarez, S. Borros, R. Kamm, D. Lauffenburger, and C. E. Semino, Tissue Eng Part A **15**, 175 (2009).
[11] V. Kumar and S. N. Upadhyay, Biotechnol. Bioeng. **101**, 843 (2008).
[12] A. I. Barakat and D. K. Lieu, Cell Biochem. Biophys. **38**, 323 (2003).
[13] See supplementary material at http://dx.doi.org/10.1063/1.3576932 for direct and indirect flow-sensing mechanisms of endothelial cells.
[14] J. Y. Park, C. M. Hwang, S. H. Lee, and S. H. Lee, Lab Chip **7**, 1673 (2007).
[15] J. Y. Park, S. K. Kim, D. H. Woo, E. J. Lee, J. H. Kim, and S. H. Lee, Stem Cells **27**, 2646 (2009).
[16] J. Y. Park, S. J. Yoo, C. M. Hwang, and S. H. Lee, Lab Chip **9**, 2194 (2009).
[17] D. E. Ingber, Semin Cancer Biol. **3**, 57 (1992).
[18] P. G. Phillips, L. M. Birnby, A. Narendran, and W. L. Milonovich, Am. J. Physiol. Lung Cell. Mol. Physiol. **281**, L278 (2001).
[19] E. Dejana, Nat. Rev. Mol. Cell Biol. **5**, 261 (2004).
[20] J. J. Feher and G. D. Ford, Am. J. Physiol. **268**, S10 (1995).
[21] L. van der Pol and J. Tramper, Trends Biotechnol. **16**, 323 (1998).
[22] S. Yedgar, N. Reisfeldgranot, and B. A. Sela, Lipids **21**, 629 (1986).
[23] H. W. Sill, Y. S. Chang, J. R. Artman, J. A. Frangos, T. M. Hollis, and J. M. Tarbell, Am. J. Physiol. Heart Circ. Physiol. **37**, H535 (1995).
[24] A. M. Malek and S. Izumo, J. Cell Sci. **109**, 713 (1996).
[25] S. Noria, D. B. Cowan, A. I. Gotlieb, and B. L. Langille, Circ. Res. **85**, 504 (1999).
[26] S. Akimoto, M. Mitsumata, T. Sasaguri, and Y. Yoshida, Circ. Res. **86**, 185 (2000).
[27] K. Matter and M. S. Balda, Nat. Rev. Mol. Cell Biol. **4**, 225 (2003).
[28] M. Ziche and L. Morbidelli, J. Neuro-Oncol. **50**, 139 (2000).
[29] V. Ralevic and G. Burnstock, Circulation **84**, 1 (1991).
[30] G. Burnstock, J. Anat. **194**, 335 (1999).
[31] J. W. Song, W. Gu, N. Futai, K. A. Warner, J. E. Nor, and S. Takayama, Anal. Chem. **77**, 3993 (2005).
[32] J. W. Song, S. P. Cavnar, A. C. Walker, K. E. Luker, M. Gupta, Y. C. Tung, G. D. Luker, and S. Takayama, PLoS ONE **4**, e5756 (2009).